THE JOURNAL OF PHYSICAL CHEMISTRY B

Article

pubs.acs.org/JPCB

Specific and Cooperative Interactions between Oximes and PAMAM Dendrimers As Demonstrated by ^{1}H NMR Study

Seok Ki Choi,*[,†] Thommey P. Thomas,[†] Pascale Leroueil,[†] Alina Kotlyar,[†] Abraham F. L. Van Der Spek,[†,§] and James R. Baker, Jr.*[,†,‡]

[†]Department of Internal Medicine, Michigan Nanotechnology Institute for Medicine and Biological Sciences, [‡]Department of Biomedical Engineering, and [§]Department of Anesthesiology, University of Michigan, Ann Arbor, Michigan 48109, United States

Supporting Information

ABSTRACT: Oximes are important in the treatment of organophosphate (OP) poisoning, but have limited biological half-lives. Complexing these drugs with a macromolecule, such as a dendrimer, could improve their pharmacokinetics. The present study investigates the intermolecular interactions that drive the complexation of oxime-based drug molecules with fifth generation poly(amidoamine) (PAMAM) dendrimers. We performed steady-state binding studies of two molecules, pralidoxime and obidoxime, employing multiple NMR methods, including 1D titration, ^{1}H−^{1}H 2D spectroscopy (COSY, NOESY), and ^{1}H diffusion-ordered spectroscopy (DOSY). Several important insights were gained in understanding the host−guest interactions occurring between the drug molecules and the polymer. First, the guest molecules bind to the dendrimer macromolecule through a specific interaction rather than through random, hydrophobic encapsulation. Second, this specificity is driven primarily by the electrostatic or H-bond interaction of the oxime at a dendrimer amine site. Also, the average strength for each drug and dendrimer interaction is affected by the surface modification of the polymer. Third, individual binding events between oximes and a dendrimer have a negative cooperative effect on subsequent oxime binding. In summary, this report provides a novel perspective important for designing host systems for drug delivery.

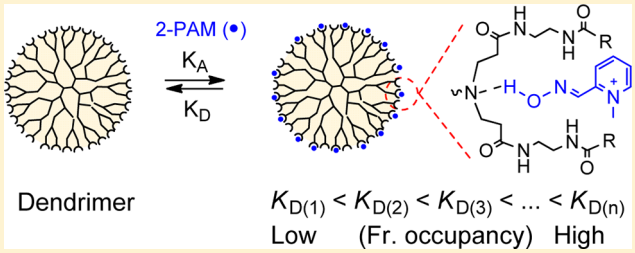

INTRODUCTION

Dendrimers belong to a family of nanometer-sized spherical macromolecules that are characteristically designed to have a well-defined core−shell architecture providing an array of repetitive cavities and branches.[1−3] The combination of such supramolecular architectures and their variable structural features has inspired a wide range of functional dendrimers as applied in the fields of catalyst design,[4−8] drug complex formation,[9−13] and multivalent ligand presentation for targeted drug delivery.[14−20] Of particular interest, the dendrimer macromolecule is able to encapsulate guest molecules and can serve as a multivalent host system that interacts simultaneously with multiple guest molecules.[21,22] The ability of dendrimers to complex small molecule drugs has been explored with a diverse array of guest molecules for biomedical and therapeutic applications, and provides for increased solubility, extended drug release kinetics,[23−27] greater serum stability of peptides and proteins,[28,29] and the intracellular transfer of siRNAs[30] and therapeutic genes.[31−33] Despite the potential utility of such applications, the basic principles that define the multivalent host−guest interactions remain poorly investigated. Only a few studies provide valuable insights on the physical basis of these interactions, and these suggest involvement of ionic associations,[34] hydrogen bonding,[21,35] hydrophobic interactions,[36,37] and $\pi-\pi$ interactions.[38,39]

In a recent communication,[9] we reported that a fifth generation (G5) PAMAM dendrimer forms complexes with the oxime-based guest molecules pralidoxime (2-PAM) and obidoxime (Figure 1). Our interest in such oxime molecules is motivated primarily by the unmet needs that relate to their undesirable pharmacokinetic profiles and their therapeutic importance. Both belong to a class of small molecules developed for the treatment of organophosphate (OP) poisoning, which is caused by the irreversible inactivation of acetylcholine esterase (AChE) as the result of a covalent reaction with the reactive OP nerve agent at the enzyme catalytic site.[40,41] The therapeutic efficacy displayed by this class of oxime molecules is attributed primarily to their ability to catalyze the reactivation of the OP-inactivated AChE. However, both drug molecules suffer an extremely short duration of action because of their rapid renal excretion ($t_{1/2} \approx 1.5-2$ h in human plasma).[42] We envisioned that complexing these oxime drug molecules into the dendrimer carrier could serve as a strategy to extend their plasma duration through a mechanism of release kinetics so that loaded drug molecules are released over the period of the long circulation half-life (≥24 h) of the dendrimer.[43−45] In our study,[9] we demonstrated that the drug−

Received: June 14, 2012
Revised: August 4, 2012
Published: August 7, 2012

   dx.doi.org/10.1021/jp305867v | J. Phys. Chem. B 2012, 116, 10387−10397

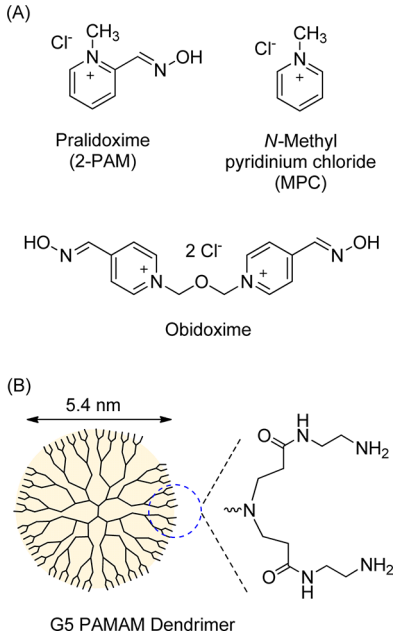

Figure 1. (A) Structures of pralidoxime (2-PAM), obidoxime, and *N*-methylpyridinium chloride (MPC). (B) The structural model of a fifth generation (G5) poly(amidoamine) (PAMAM) dendrimer. The theoretical number of amine-terminated branches per dendrimer is 128, but only a fraction of the branches is shown for clarity.

dendrimer complexes form in a specific manner, wherein each oxime molecule interacts through the electrostatic attraction mechanism with the primary amine terminated at the peripheral branch.

Here, we report a complete analysis of the forces underlying the complexation of 2-PAM and obidoxime with G5 PAMAM dendrimers. This study focuses on structural variations in the G5 PAMAM dendrimers (Figure 2). First, we investigated the location and mechanism by which oxime molecules are able to complex with each surface-modified dendrimer. In contrast to the ionic interaction observed with the amine-surfaced PAMAM dendrimers, oxime molecules employ a different mechanism for interaction with the surface-modified dendrimers by binding at other nonprimary amine sites. We also investigated binding cooperativity that controls the strength of individual host−guest interactions occurring with the dendrimer. Our analysis suggests that individual binding events lead to a distribution of affinities that decrease as the number of interactive oximes increases. In summary, the present study describes the quantitative interaction of dendrimers with oxime drugs and proposes mechanistic insights that are of fundamental value for understanding host−guest interactions in drug carrier systems.

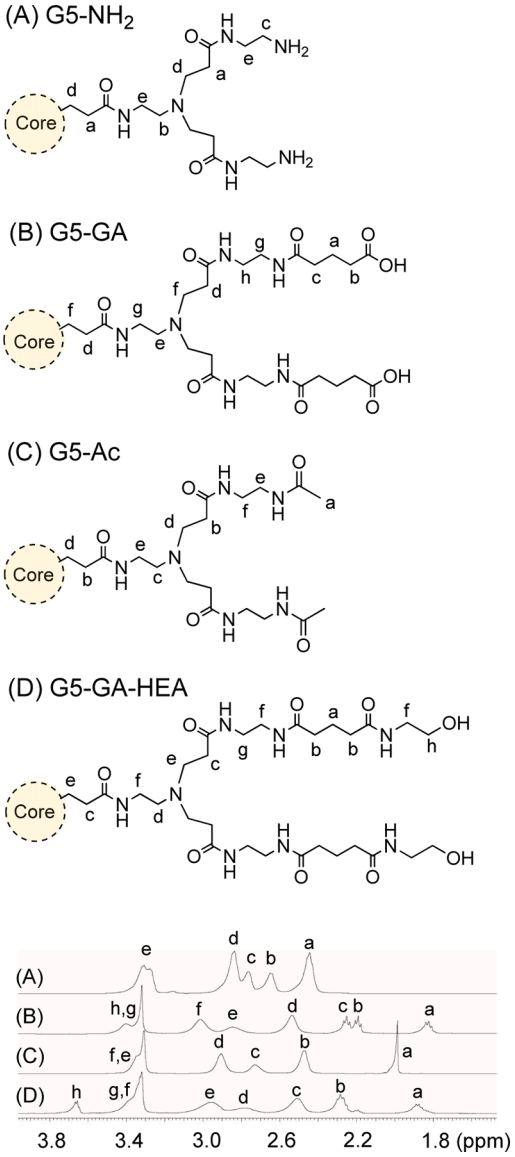

Figure 2. (Top) Peripheral branches and their proton labeling systems for G5 PAMAM dendrimer (G5-NH_2), and its surface modified dendrimers (G5-Ac, G5-GA, and G5-GA-HEA). Those functional groups used for the modification of dendrimer branches include acetamide (Ac), glutaric acid (GA), or glutaric acid 2-hydroxylethylamide (GA-HEA). The protons of interest for each terminal branch are labeled in alphabetical order starting with the protons that appear at the most upfield region in the ^{1}H NMR spectrum. Given the symmetry of the dendrimer structure, only a single set of the protons from the two identical branches are illustrated for clarity. (Bottom) ^{1}H NMR spectra of these four dendrimers, each taken in D_2O (5 mg/mL), are overlaid for comparison.

MATERIALS AND METHODS

Materials. All of the reagents and chemicals were purchased from Sigma-Aldrich unless noted otherwise. Deuterium oxide (99.9 atom % D) used for the NMR study contains 0.05 wt % of 3-(trimethylsilyl)propionic-2,2,3,3-d_4 acid sodium salt as an internal standard. Pralidoxime chloride (pyridine-2-aldoxime methochloride, 99%) and obidoxime chloride (≥95%) were used as received. Deuterated phosphate-buffered saline (PBS) solution was prepared by dissolving the PBS powder in deuterium oxide at the concentration of 1 × PBS (phosphate 0.01 M, NaCl 0.138 M, KCl 0.0027 M, pH 7.4) following the instruction on the powder pouch. G5 PAMAM dendrimer (G5-NH_2) was purchased as a 17.5% (w/w) methanol solution (Dendritech, Inc., Midland, MI), and purified by dialysis prior to use as described elsewhere.[9,46] The average number (n) of primary amines per dendrimer molecule G5-$(NH_2)_n$ was determined by the potentiometric titration method[14] by using a Mettler Toledo MP230 pH meter equipped with an InLab Micro electrode at RT (23 ± 1 °C). The average number (n) was determined as 114 from the back-titration data. Two surface-modified dendrimers (Figure 2) were prepared from the parent G5-NH_2 following the standard methods that include a

dx.doi.org/10.1021/jp305867v | J. Phys. Chem. B 2012, 116, 10387−10397

fully acetylated neutral dendrimer (G5-Ac; Figure 2C)[14] and a fully glutaric acid-terminated anionic dendrimer (G5-GA; Figure 2B).[46] Each modified dendrimer was purified by successive membrane dialysis (Spectrum Laboratories; MWCO 10 000) against the PBS solution (2 × 12 h) and deionized water (2 × 12 h). Thus, the G5-GA batch prepared in this study presents its terminal carboxylic acid primarily as its sodium salt form. Another surface-modified dendrimer G5-GA-HEA (Figure 2D) was prepared from G5-GA by amide formation at each glutaric acid to 2-hydroxyethylglutaryl amide:[46,47] (i) EDC (2.0 equiv), NHS (1.1 equiv), DMAP (2.0 equiv), DMF, RT, 24 h; (ii) 2-aminoethanol (228 equiv), RT, 12 h where each equiv is relative to the glutaric acid moiety. This G5-GA-HEA dendrimer was also purified by the dialysis method as described above. Each of the dendrimers was fully characterized by a number of standard analytical methods including high performance liquid chromatography (HPLC), gel permeation chromatography (GPC), matrix-assisted laser desorption ionization-time-of-flight (MALDI TOF) mass spectrometry, and ^{1}H NMR spectroscopy as described earlier.[9]

General NMR Spectroscopy. All NMR experiments for the oxime drug titration and two-dimensional (2D) spectroscopy (COSY, NOESY) were performed as described previously at 499.9 MHz (11.7 T) for ^{1}H nucleus using a Varian NMR spectrometer equipped with Performa I, *Z*-axis pulsed field gradient module and automatic gradient shimming module.[9] Diffusion-ordered spectroscopy (DOSY) was carried out at 499.9 MHz (11.7 T) using the NMR spectrometer equipped with a pulsed field gradient (62 G/cm) amplifier, and a dual channel protune module. Values for chemical shift (δ) in each ^{1}H NMR spectrum are reported in ppm relative to an internal standard, 2,2-dimethyl-2-silapentane-5-sulfonate sodium salt (DSS; δ = 0.00). All 1D and 2D experiments were performed at 297.3 K (±0.2).

^{1}H NMR Titration Experiments. The titration experiment was carried out by adding the solution of 2-PAM, obidoxime, or other control molecule in incremental amounts to the solution of G5 PAMAM dendrimer (0.55 mL) preloaded in an NMR tube. Each stock solution for the titration was prepared by dissolving the dendrimer or the oxime molecule in D_2O or deuterated PBS at the concentration specified later in each of the experiments. The titration experiment was performed in triplicate for each dendrimer−drug complex. Mole fractions for bound or free drug molecules at equilibrium were calculated by eq 1 under fast exchange conditions where an observed signal appears at the population-averaged chemical shift.[48,49]

$$\delta_{obsd} = (Fr_{free} \times \delta_{free} + Fr_{bound} \times \delta_{bound}),$$
$$\text{where } (Fr_{free} + Fr_{bound}) = 1 \quad (1)$$

The chemical shift value assigned for the free state (δ_{free}) refers to the value obtained with a free drug molecule (alone) in D_2O or the deuterated PBS solution. The chemical shift value for the bound state (δ_{bound}) is defined as the signal for a drug molecule bound to the dendrimer where the ratio of [drug]/[dendrimer] is 1 or less than 5. Those protons selected for the fractional analysis of the 2-PAM binding include H_1 (N-CH_3), H_2, H_3, and H_6 (Figure 3). Those protons selected for the obidoxime analysis include H_2, H_3, and H_4 (Figure 4). In a typical analysis, the fraction of bound drug molecules was determined for each select proton, and an average value was calculated from those selected protons. Each value reported for the fraction of bound drug molecules, or the fraction of occupied binding sites, refers to the mean of three independent sets of titration data. The uncertainty value associated with the measurement of chemical shift (δ) was ±0.002 ppm.

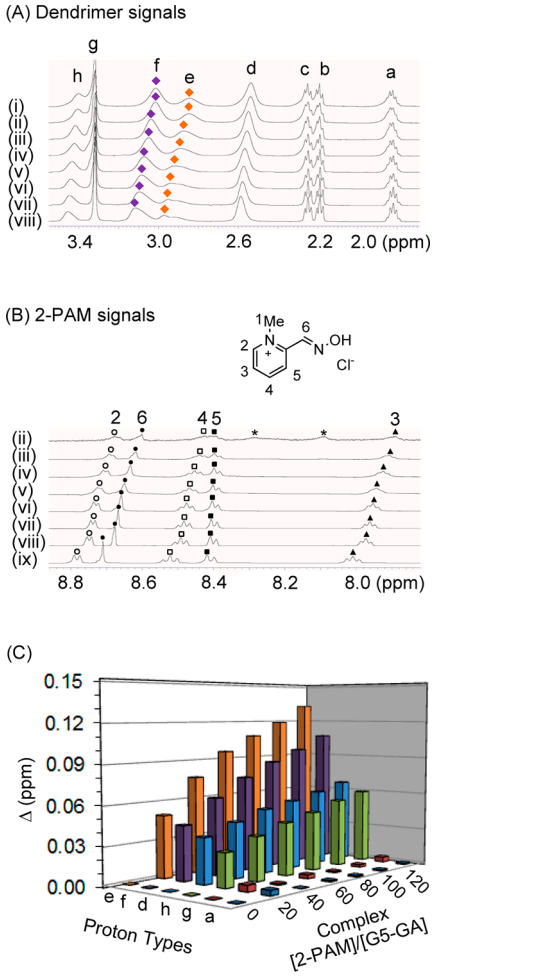

Figure 3. ^{1}H NMR titration experiments for the complex formation between the glutaric acid-terminated dendrimer (G5-GA) and pralidoxime chloride (2-PAM) in D_2O. ^{1}H NMR spectral regions are shown separately for the dendrimer G5-GA (A), and 2-PAM (B). G5-GA alone (6.23×10^{-4} M) (i), and the dendrimer−drug complexes, each prepared at [2-PAM]/[G5-GA] = 1 (ii), 10 (iii), 20 (iv), 40 (v), 60 (vi), 80 (vii), 120 (viii), and 2-PAM alone (ix). The signals marked with * (8.1−8.3 ppm) are attributed to the internal amide (NH) protons of the dendrimer molecule that are resistant against the H−D exchange with solvent molecules. (C) Changes in chemical shift values (e.g., Δ for f protons = ($\delta_{f,viii} - \delta_{f,i}$) ppm) plotted as a function of [2-PAM]/[G5-GA] ratio, and measured for the select type of the dendrimer protons.

Two-Dimensional (2D) NMR Spectroscopy. The 2D experiments for dendrimer−oxime drug complexes were performed as described earlier.[9] The ^{1}H−^{1}H COSY experiment was performed under following acquisition parameters: ^{1}H pulse width (pw) = 7.9 μs; relaxation delay (d_1) = 1 s; acquisition time = 0.15 s; number of scans per t_1 increment = 2; number of t_1 increment = 128. The data acquisition for 2D ^{1}H−^{1}H NOESY experiments was carried out at the NOE mixing time of 200 ms, 10.44 μs of ^{1}H pulse width, relaxation delay of 2 s, and acquisition time of 0.2 s. Eight transients were averaged per t_1 increment, and number of t_1 increment was 128. Each of the 2D spectral data was processed using Varian's Vnmr J software.

dx.doi.org/10.1021/jp305867v | J. Phys. Chem. B 2012, 116, 10387−10397

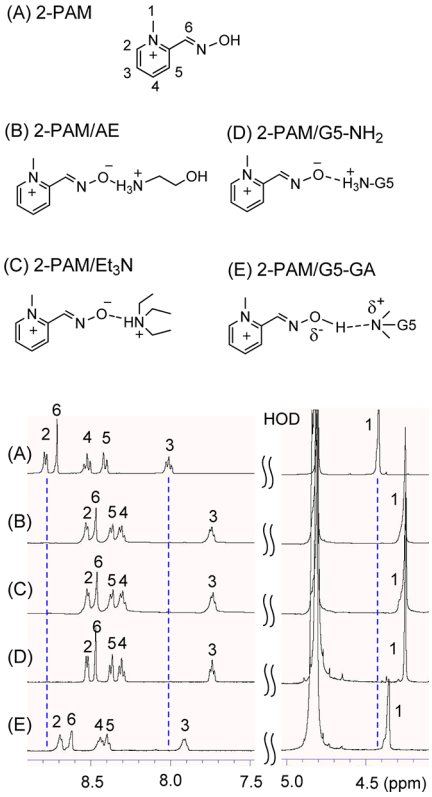

Figure 4. ^{1}H NMR spectral signals for pralidoxime chloride (2-PAM) acquired as different forms. The drug alone in D_2O (6.0×10^{-2} M, A), the drug mixed with 1 mol equiv of 2-aminoethanol (B), or triethylamine (C), and the drug in complex with G5-NH_2 (6.2×10^{-4} M) (D), and G5-GA (5.5×10^{-4} M) (E) where the molar ratio of 2-PAM to each dendrimer molecule is 10.

Diffusion-Ordered Spectroscopy (DOSY). DOSY experiments for PAMAM dendrimers (G5-NH_2, G5-Ac, G5-GA, and G5-GA-HEA) were performed at the dilute concentration, each prepared in D_2O (1.2 mg/mL). DOSY experiments for the G5-GA/2-PAM complexes were performed at [G5-GA] = 1.2 mg/mL and the ratio of [2-PAM]/[G5-GA] = 40, or 80. Each experiment was carried out using the DOSY gradient compensated stimulated echo with spin lock and convection compensation (DgcsteSL_cc) as described earlier.[9] This method represents an enhancement of the classical pulsed gradient spin–echo (PGSE) pulse sequence,[50] and its acquisition parameters include 15 increments in the gradient strength, 2.0 ms of diffusion gradient length, and 200 ms of diffusion delay. Calibration of the instrument was performed with D_2O at 290 K to G/cm (0.009 61 G/(cm × DAC)). DOSY spectral data were processed using VnmrJ software, and diffusion coefficient (D, m^2 s^{-1}) for the dendrimer alone or the drug complex was determined by using a default method in the software. This method is based on fitting of the integration of the dendrimer peak to the Stejskal–Tanner function[51] (eq 2) where the magnetogyric constant (γ) of ^{1}H nucleus is 2.675 × 108 T^{-1} s^{-1}.

$$\ln(I/I_0) = -\gamma^2\delta^2G^2(\Delta - \delta/3)D \quad (2)$$

Each diffusion coefficient is reported as a mean value obtained from at least three independent sets of measurement, and the error is expressed as the standard deviation from the mean value.

In Vitro Cytotoxicity Assay. Cytotoxicity of G5 PAMAM dendrimers was evaluated in two mammalian cell lines including KB cells, a subline of the cervical carcinoma HeLa cells, and the mouse melanoma B16–F10 cell line as described elsewhere.[52] The cells were grown as monolayer cell culture at 37 °C and 5% CO_2 in RPMI medium (folate-free for the KB cells) supplemented with 10% fetal bovine serum. The cells were seeded in 96-well microtiter plates (3000 cells/well). Two days after plating, the cells were treated with the dendrimer conjugates in tissue culture medium for 3 days. A colorimetric "XTT" (sodium 3-[1-(phenylaminocarbonyl)-3,4-tetrazolium]-bis(4-methoxy-6-nitro)benzenesulfonic acid hydrate) assay[53] (Roche Molecular Biochemicals, Indianapolis, IN) was performed, following the vendor's protocol. After incubation with the XTT labeling mixture, the microtiter plates were read on an ELISA reader (Synergy HT, BioTek) at 492 nm with the reference wavelength at 690 nm.

RESULTS AND DISCUSSION

Surface Modification of G5 PAMAM Dendrimer. In our earlier study with the unmodified G5 PAMAM dendrimer (G5-NH_2), we demonstrated that the complexation with 2-PAM and obidoxime molecules occurs through the ionic interaction at the dendritic primary amine terminated at the peripheral branch.[9] The present study extends the scope and perspective of the oxime complexation by investigation of how the surface property of the PAMAM dendrimer affects the complexation. Several studies already suggest that the surface modification of the dendrimers alters the chemical and physical property of the surface, and as a result can affect the modes of interaction with guest molecules.[23,37] Thus, our primary objective for testing the surface modification is to understand how it impacts the binding of the oxime drug molecules to the dendrimer structure where primary amine branches are not available. To address

Table 1. Molecular Properties of Four PAMAM Dendrimers and Two Oxime Antidote Molecules Used in the Present Study

molecules	mol wt (g mol^{-1})	PDI[c]	no. of terminal branches	terminal functional group	pK_a[g]
G5-NH_2	27600[a] (26270[b])	1.010	114[d] (128[e])	$-NH_2$	9.0–10.77 (refs 56, 57)
G5-Ac	33100[a] (28140[b])	1.016	114[f]	−NHAc	15.67[h] (NH)
G5-GA	40200[a] (40850[b])	1.046	108[f]	−COOH	4.59[h]
G5-GA-HEA	42840[b]	1.105	108[f]	$-CONH(CH_2)_2OH$	14.17[h] (NH)
pralidoxime (2-PAM)	137.1	–	–	=NOH	8.1 (ref 55)
obidoxime	288.1	–	–	=NOH	8.0 (ref 58)

[a]Measured by matrix-assisted laser desorption ionization (MALDI) mass spectrometry. [b]Number-averaged molecular weight (M_n) determined by gel permeation chromatography. [c]Polydispersity index (PDI) = M_w/M_n. [d]Mean number determined by the potentiometric titration method. [e]Theoretical number. [f]Mean number determined by the ^{1}H NMR method. [g]Value for the terminal group. [h]Calculated by Advanced Chemistry Development (ACD/Laboratories) Software V8.14.

dx.doi.org/10.1021/jp305867v | J. Phys. Chem. B 2012, 116, 10387–10397

this effect, we selected three types of the G5 PAMAM dendrimer, each derived from the identical batch of G5-NH_2 but with distinct derivatization at the terminal amine. These dendrimers include a fully acetylated dendrimer (G5-Ac),[14] a fully glutaric acid-terminated dendrimer (G5-GA),[46] and a glutaryl hydroxyethylamide-terminated dendrimer (G5-GA-HEA) (Figure 2). This selection is not extensive but still allows the investigation of the effect of surface modification while other structural parameters remain intact such as the dendrimer generation, and the structural integrity of inner branches and cavities.

Each of these PAMAM dendrimers was prepared following a standard modification method described elsewhere,[14,46,47] and fully characterized as summarized in Table 1 (MALDI-TOF), Figure 2 (^{1}H NMR), and Figure S1 (Supporting Information; GPC). In addition to the physicochemical analysis, we also determined if such surface modification alters the biological property of the parent G5-NH_2, the polycationic dendrimer which is toxic to mammalian cells.[52,54] Evaluation of the cytotoxicity of the PAMAM dendrimers was performed in two mammalian cell lines including KB cells, and the mouse melanoma B16−F10 cell line as described elsewhere.[52] In consistency with the prior result,[52] the positively charged G5-NH_2 showed a dose-dependent cytotoxicity in both cell lines (Figure S2 in the Supporting Information). In contrast, all the other surface-modified dendrimers were not cytotoxic in both cell lines tested under otherwise the identical condition and doses of up to 3000 nM (Figure S2). Thus, modification of the cationic surface to the neutral or negatively charged one abolishes the undesired cell toxicity associated with the unmodified G5-NH_2, and provides higher level of biocompatibility as reported elsewhere.[14,45]

Complexation of 2-PAM with G5-GA. First, we performed ^{1}H NMR titration experiments for evaluating the complex formation between the glutaric acid-terminated dendrimer G5-GA and 2-PAM in D_2O (Figure 3). This binding study enables to locate structural determinants involved in the complex formation between the dendrimer and the oxime molecule. Upon addition of 2-PAM made in a titration manner, certain subsets of the dendrimer protons shifted downfield as a function of the [2-PAM]/[G5-GA] ratio. Such shift occurred at those protons (e, f, d, h) that are in close proximity to the tertiary amine flanked with two identical glutaric acid-terminated branches. Otherwise inner protons and other outer protons that constitute the glutaric acid residue remained almost unchanged. The magnitudes of such shifts (Δ) are variable and greater in particular for those protons attached to the carbon adjacent directly to the tertiary nitrogen (Δ: e > f > d ≈ h). It suggests that the guest oxime molecules selectively bind at such tertiary amine sites within the dendrimer. On the guest side (2-PAM), its proton signals underwent the upfield shift in a manner which increases as a function of the [G5-GA]/[2-PAM] ratio (Figure 3b).

Mode of Interaction. In the prior study performed with G5-NH_2,[9] we hypothesized that electrostatic interaction is the driving force for the binding of the 2-PAM molecule (pK_a of −NOH = 8.1[55]) to the terminal primary amine (pK_a = 9.0[56]−10.77[57] for its conjugated acid). One of the experiments we performed for verifying this interaction model was to compare reference 2-PAM solutions, each prepared in a relevant salt form by mixing with an equimolar amount of a small amine molecule having the same basicity. Figure 4 compares selected regions of these ^{1}H NMR spectral signals for 2-PAM in complex with triethylamine (pK_a = 10.78), ethanolamine (pK_a = 9.50), G5-NH_2, and G5-GA (see Figure S3 in the Supporting Information for full spectra). The 2-PAM drug molecule mixed with each of these basic amines shows the upfield shift compared to the drug alone. In addition, the difference (Δ) in the chemical shift value for each 2-PAM proton was almost identical to the Δ value observed in a bound state with G5-NH_2 ([2-PAM]/[G5-NH_2] = 10). This NMR signature suggests that 2-PAM binding to G5-NH_2 occurs via the electrostatic mechanism.

Interestingly, 2-PAM in complex with G5-GA at [2-PAM]/[G5-GA] = 10 also shows the upfield shift, but such shift is smaller than the shift observed from the complexes made with those small amine molecules or G5-NH_2. This distinct NMR shift suggests that 2-PAM binds to the G5-GA dendrimer through a different mode of interaction because this modified dendrimer lacks the primary amine required for the full ionic interaction. On the basis of the NMR titration experiment, we hypothesize that the tertiary amine group serves as the individual receptor site for the oxime drug molecule, and the primary interaction occurs between the tertiary nitrogen and the oxime moiety (=NOH). However, the basicity of the tertiary amine for this dendrimer (pK_a = 6.3−6.85 for its conjugate acid[57]) is not sufficiently strong for full deprotonation of the oxime proton (=NOH; pK_a = 8.1[55]). Thus, we hypothesize that the drug binding occurs instead through the H-bond, or partial ionic interaction that does not involve a full charge separation.

We further confirmed that the oxime functionality (=NOH) of 2-PAM plays a key role in binding the G5-GA site by using *N*-methylpyridinium chloride (MPC, Figure 1), a comparator molecule that lacks such an essential aldoxime moiety. The ^{1}H NMR titration experiment performed under otherwise an identical condition provided no evidence supportive of the interaction between the MPC molecule and the G5-GA dendrimer because neither the MPC nor the dendrimer signals showed any noticeable changes in the chemical shift values (Figure S4 in the Supporting Information). Given that the above titration experiment with 2-PAM was performed in a nonionic solution (D_2O), we investigated whether the ionic strength of the solution influences the oxime binding or alters its mode of binding. We performed the same titration experiment in phosphate buffered saline (PBS, pH 7.4; I = 0.15) solution, and observed almost identical trends in the chemical shift as compared to the nonionic solution (Figure S4). It suggests no detrimental effect of the ionic strength to the oxime−dendrimer complexation.

Effect of Oxime Structure. We also extended the scope of drug−dendrimer complexation by varying the type of the oxime molecules. We performed the titration experiment of G5-GA with obidoxime (pK_a = 8.0),[58] the homodimeric molecule that comprises two identical units of 4-pyridinium aldoxime moiety linked through the 2-oxapropane spacer. The ^{1}H NMR spectral data in Figure 5 show signal shifts in both the dendrimer and the drug molecule, suggesting the complex formation. The dendrimer signals showed downfield shifts in response to the variation of the [obidoxime]/[G5-GA] ratio. Like the case of 2-PAM, those dendrimer protons in close proximity to the tertiary amine group showed larger shifts (Δ: e > f > d ≈ h), while other inner and outer protons remained almost unchanged. Both the coupling patterns and magnitudes of such signal shifts are consistent with those seen with 2-PAM. On the guest side, the obidoxime showed upfield shift as a

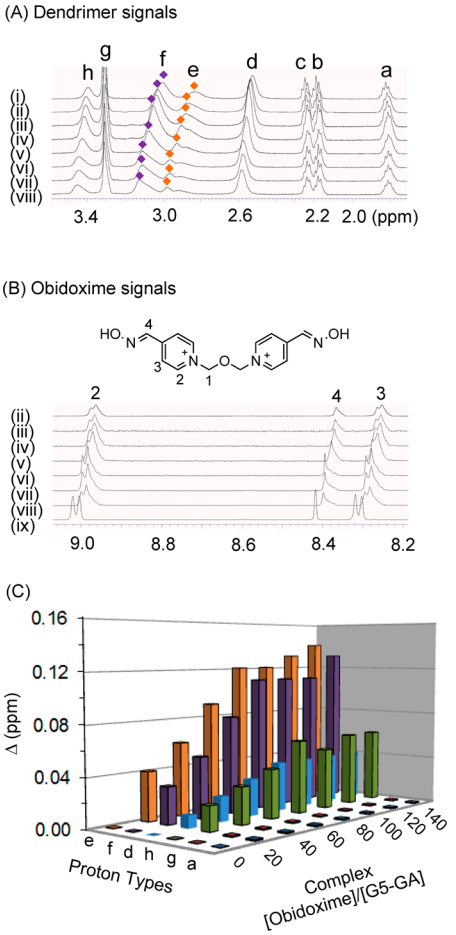

Figure 5. ^{1}H NMR titration experiments for G5-GA dendrimer with obidoxime in D_2O. The spectral regions for the glutaric acid-terminated dendrimer (A), and obidoxime (B). G5-GA dendrimer alone (2.49×10^{-4} M) (i), and dendrimer–drug complexes prepared at [obidoxime]/[G5-GA] = 10 (ii), 20 (iii), 40 (iv), 60 (v), 80 (vi), 100 (vii), 140 (viii), and obidoxime alone (ix). (C) Changes in chemical shift values (e.g., $\Delta = (\delta_{f,viii} - \delta_{f,i})$ ppm) plotted as a function of [obidoxime]/[G5-GA] ratio, and measured for the select type of the dendrimer protons.

function of the [G5-GA]/[obidoxime] ratio. This titration experiment suggests that the obidoxime molecule binds the G5-GA site as does the 2-PAM molecule on the basis of the same mode of interaction between the oxime (=NOH) and the tertiary amine group.

Proposed Models for Dendrimer–Oxime Complexation. We investigated the mode of drug complexation for two additional dendrimers G5-Ac, and G5-GA-HEA, each modified with the neutral amide group on the surface (Figure 2). By performing the titration experiments similarly, ^{1}H NMR spectral data were acquired for each complex as a function of [2-PAM]/[D] as shown in Figure S4 (in the Supporting Information) where D refers to the dendrimer. Those select dendrimer protons that underwent changes (Δ) in the chemical shift values are plotted as a function of [2-PAM]/[D] ratio (Figure S5 in the Supporting Information). In each complex, the signal shift occurs mainly with those dendrimer protons adjacent to the tertiary nitrogen. Proton signals associated with 2-PAM shifted upfield upon its complexation to the dendrimer. Thus, the G5-Ac or G5-GA-HEA dendrimer shows the similar binding patterns as observed with the G5-GA dendrimer. It suggests the same mode of binding regardless of the difference in chemical modifications made on the dendrimer surface. However, it should be noted that the shifted values (Δ) generated upon the drug complexation are much smaller for both G5-Ac and G5-GA-HEA than G5-GA (Figure S5). Such smaller shifts are qualitatively indicative of weaker interactions, and this concept is supported by more quantitative analysis to be discussed later. In summary, by performing ^{1}H NMR titration experiments, we were able to identify the primary binding motif of the dendrimer that serves the host site for interacting with oxime guest molecules (Figure 6). Each host (receptor) is composed of the tertiary amine group branched out with two terminal residues, and accordingly, a single dendrimer molecule contains approximately either 57 (G5-Ac) or 54 (G5-GA, G5-GA-HEA) copies of such receptor site, each

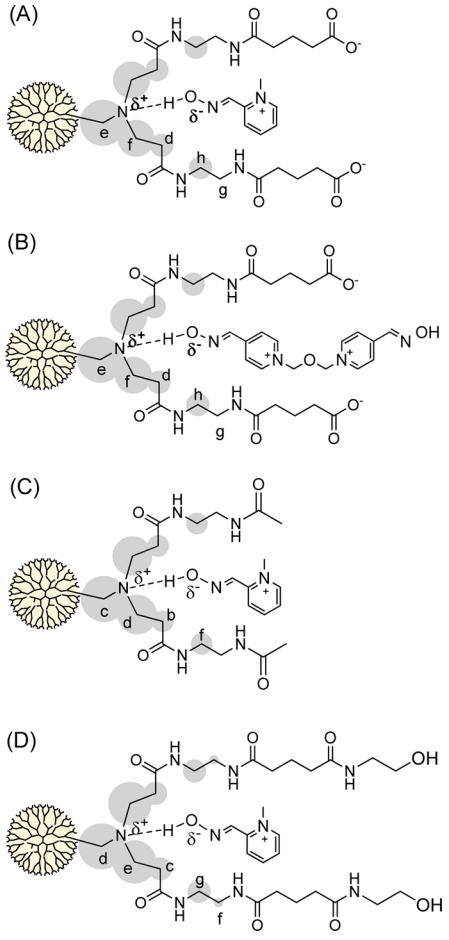

Figure 6. Proposed models for three G5 PAMAM dendrimers, each in complex with 2-PAM or obidoxime as suggested by the ^{1}H NMR titration experiments in D_2O, (A) G5-GA/2-PAM, (B) G5-GA/obidoxime, (C) G5-Ac/2-PAM, and (D) G5-GA-HEA/2-PAM. In this study, the binding site (receptor) of the dendrimer was identified as the discrete domain that shows significant changes in the chemical shift values ($\Delta = \delta_{drug\ added} - \delta_{free}$, ppm) upon addition of the oxime molecule. In each model, the receptor unit is composed of the tertiary amine group flanked with two neighboring terminal branches (shaded circles). Please note that the size of the gray circle is directly proportional to the change (Δ), and expressed relative to the proton that shows the largest change (H_e for G5-GA, H_c for G5-Ac, and H_d for G5-GA-HEA). Note that H–D exchangeable protons and those that show less than 5% of the changes are not indicated for clarity.

dx.doi.org/10.1021/jp305867v | J. Phys. Chem. B 2012, 116, 10387–10397

number referring to half the total number of terminal branches per dendrimer (Table 1).

2D NMR Spectroscopy. Evidence for the binding model of G5-GA as proposed in Figure 6 was further investigated by 2D NMR techniques. We performed ^{1}H−^{1}H COSY and NOESY NMR experiments, each for the G5-GA dendrimer complex made with either 2-PAM (Figure 7) or obidoxime (Figure S6 in the Supporting Information). The ^{1}H−^{1}H COSY spectrum for the 2-PAM complex confirms the bond connectivity among multiple sets of spin−spin coupled protons that belong to either the oxime molecule or the dendrimer (Figure 7A,B). Specifically, those cross peaks marked in each spectral region enable to correctly assign and correlate various proton signals from the dendrimer and the drug molecule. The NOESY spectrum acquired for the same complex solution shows certain cross peaks between CH_3 protons (2-PAM) and g protons (G5-GA) as the result of the NOE effect attributed to through-space intermolecular correlation. This provides evidence for spatial proximity ($d \leq 5$ Å) between the oxime molecule and the dendrimer site made of the tertiary amine moiety (Figure 6). The COSY experiment performed for G5-GA dendrimer in complex with obidoxime also enabled us to correctly assign proton signals for the obidoxime molecule (Figure S6). Its NOESY cross peaks indicate the correlation between the H_2 protons (obidoxime) and the g protons (dendrimer), and support the intermolecular interaction between the obidoxime molecule and the dendrimer site (Figure 6).

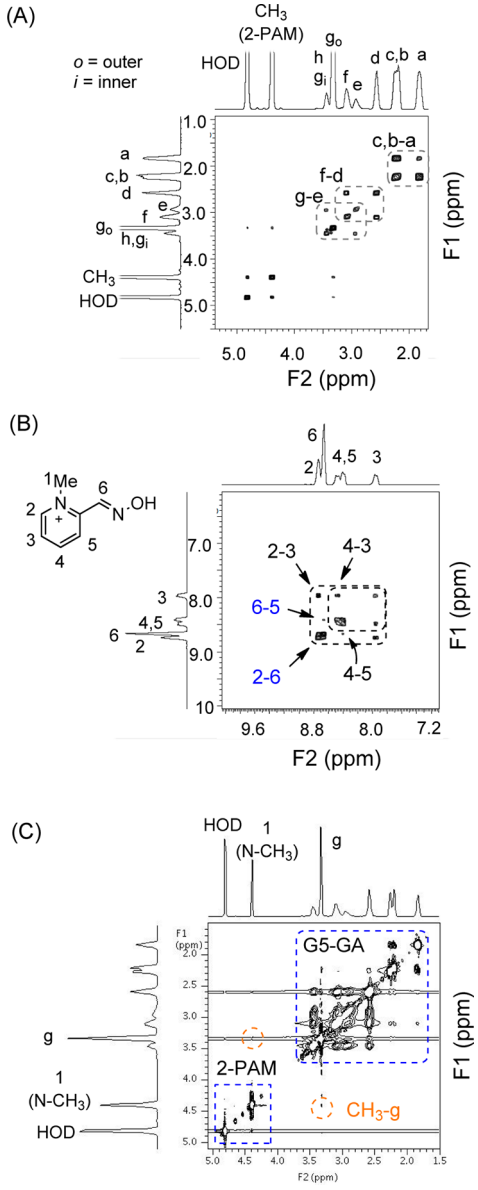

Figure 7. Two-dimensional (2D) ^{1}H NMR spectra for G5-GA dendrimer in complex with 2-PAM in D_2O ([D] = 5.47 × 10^{-4} M; [2-PAM]/[D] = 80). (A,B) ^{1}H−^{1}H COSY spectrum: spectral features are shown separately for the dendrimer region, and the 2-PAM region. Cross peaks in the dashed rectangles indicate the scalar coupling between the marked protons from either 2-PAM or the dendrimer. (C) ^{1}H−^{1}H NOESY spectrum: cross peaks shown in the dashed rectangles indicate the through-space intramolecular correlation, and those in the dashed circle indicate the intermolecular correlation between the 2-PAM proton (H_1 = CH_3) and the dendrimer protons (g).

Diffusion-Ordered Spectroscopy. We studied hydrodynamic properties of the G5-GA complexes made with 2-PAM in the aqueous solution by performing ^{1}H diffusion-ordered spectroscopy (DOSY)[59] experiments (Figure 8, and Figure S7 in the Supporting Information). As described in detail earlier in the Materials and Methods section, we fitted the peak-integration decay curves of the DOSY spectra (Figure S7) according to the Stejskal−Tanner function[51] (eq 2), and determined diffusion coefficients (D, m^2 s^{-1}) for the dendrimer alone or its PAM complex. The diffusion coefficients determined here by this NMR method were then used to calculate hydrodynamic radii (R_h) for the dendrimers or the complexes according to the Einstein−Stokes equation (eq 3, where η is viscosity of D_2O = 1.24 × 10^{-3} kg m^{-1} s^{-1}, $\kappa\varphi \ll 1$ for the dilute solutions, and other parameters as defined in the literature[11,30]).

$$D = k_B T(1 - \kappa\varphi)/6\pi\eta R_h \quad (3)$$

Figure 8B shows the plot of diffusion coefficients presented with regard to the structure of G5 PAMAM dendrimers. It demonstrates that the diffusivity varies in response to the surface modification such as the size and charge of the modifying group. Relative to the parent G5-NH_2 (D = 7.49 (±0.30) × 10^{-11} m^2 s^{-1}),[9] the derivatization at the primary amine decreases the diffusion coefficient as illustrated by G5-Ac (6.86 × 10^{-11} m^2 s^{-1}), G5-GA (5.24 × 10^{-11} m^2 s^{-1}), and G5-GA-HEA (5.91 × 10^{-11} m^2 s^{-1}). Values of hydrodynamic radius (R_h) for the dendrimers are also plotted in Figure 8B which are inversely correlated with diffusion coefficients (eq 3): G5-NH_2 (2.35 nm), G5-Ac (2.56 nm), G5-GA (3.36 nm), and G5-GA-HEA (2.98 nm). Interestingly, the negatively charged dendrimer G5-GA has a hydrodynamic radius slightly larger than G5-GA-HEA, the neutral dendrimer which is derived directly from G5-GA by further derivatization at each glutaric acid (GA) to the 2-hydroxyethylamide (GA-HEA). This inconsistency in the correlation of the hydrodynamic radius to the size of the structural modification is likely attributable to the contribution of the surface charge of the G5-GA dendrimer. In an earlier study by Tomalia et al.,[60] an electrical double layer model was proposed for the negatively charged dendrimer particles where both counter cations and water molecules are strongly associated with the carboxylate anions present on the dendrimer surface. So, the hydrodynamic radius measured experimentally for the G5-GA dendrimer reflects not only the increased size of the attached GA groups but also the electrical double layer associated with the charged residues.

dx.doi.org/10.1021/jp305867v | J. Phys. Chem. B 2012, 116, 10387−10397

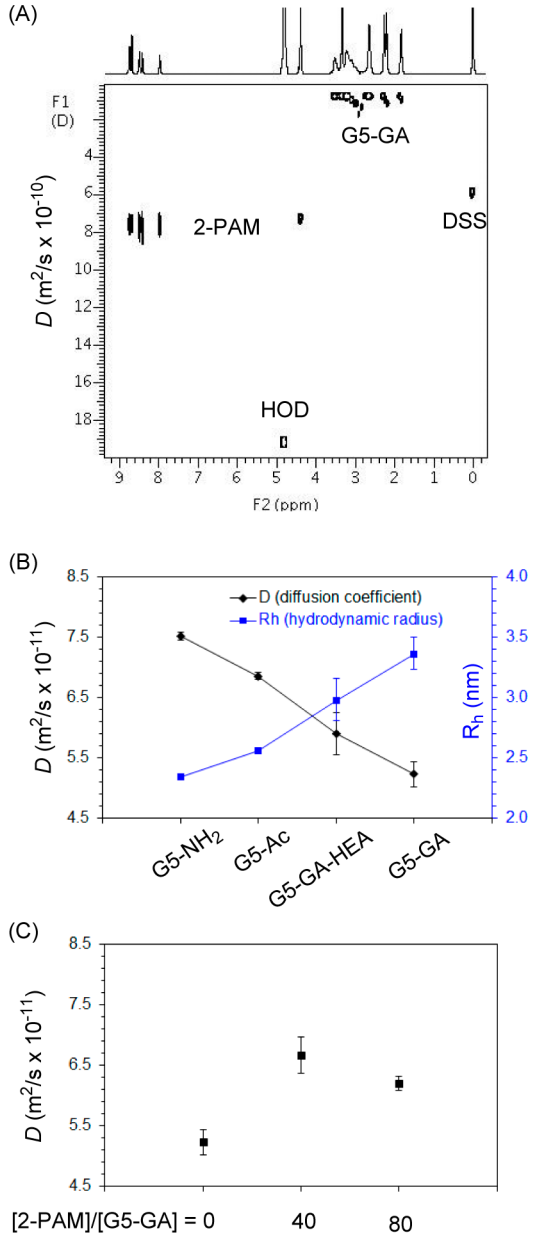

Figure 8. (A) A representative pseudo-2D DOSY plot for G5-GA dendrimer in complex with 2-PAM ([G5-GA] = 4.15×10^{-5} M; [2-PAM]/[G5-GA] = 80). (B) Diffusion coefficients (D, m^2 s^{-1}), and hydrodynamic radii (R_h, nm), each plotted for a fifth generation PAMAM dendrimer (G5-NH_2), and three modified dendrimers, G5-Ac, G5-GA-HEA, and G5-GA. (C) Diffusion coefficients (D) for G5-GA alone, or in complex with 2-PAM, each complex prepared at two [2-PAM]/[G5-GA] ratios (= 40, 80). Diffusion coefficient reported for each dendrimer or its drug complex refers to a mean value obtained from at least three independent sets of measurements, and the error represents the standard deviation from the mean value.

Next, we performed the same DOSY experiments to investigate whether the complexation of the G5-GA dendrimer with 2-PAM molecules influences the diffusion coefficient of the resulting complex. As shown in Figure 8C, two complexes, each prepared at a different [2-PAM]/[G5-GA] ratio = 40 and 80, display diffusion coefficients which are greater than the value acquired with the G5-GA dendrimer alone. Such difference supports the formation of the complexes as proposed by the titration and 2D NMR experiments. This observation is quite interesting because the diffusivity increases upon the complex formation. We believe that such increase might be attributable to the partial neutralization of the negative charges of the dendrimer by the positively charged pyridinium ions (2-PAM) colocalized at the surface.

Fractional Occupancy (θ). In order to quantitatively understand the physical basis of individual binding events that constitute the global complexation, we calculated the fractions of drug molecules bound, and in a complementary manner, the fractions of occupied binding sites (θ) by analyzing the ^{1}H NMR titration data (Figures 3B and 5B, and Figure S4 in the Supporting Information). According to the chemical shift changes as discussed in the titration experiments, each drug molecule undergoes fast on/off exchange, and its signal appears at the population-averaged chemical shift instead of distinct signal peaks for bound and free molecules.[48,49] Therefore, the present dendrimer−oxime complexation could be analyzed by eq 1 which is established for such a fast exchange system. As described in the Materials and Methods section, we determined molar fractions of oxime drug molecules bound for each dendrimer complex according to eq 1,[48] and used the resultant values for calculating the corresponding fractions of receptor occupancy (θ) which we define as the number of occupied sites (=drug molecules bound) relative to the total number of binding (receptor) sites available per dendrimer (Table 1, Figure 6).

Figure 9 summarizes the fractional occupancy (θ) for the dendrimer−oxime complexes made with G5-GA, G5-Ac, and G5-GA-HEA, each plotted as a function of the [oxime]/[D] ratio where oxime refers to 2-PAM or obidoxime and D refers to the dendrimer. In general, it illustrates that the fractional occupancy increases nonlinearly in response to the [oxime]/[D] ratio. However the maximal fractional occupancy is greater for the complex with G5-GA ($\theta \approx 0.8-0.9$) than with the other dendrimers ($\theta \approx 0.3$) such as G5-Ac and G5-GA-HEA. Specifically, 2-PAM in D_2O shows the θ value of 0.54 at [2-PAM]/[G5-GA] = 60, indicating that approximately 30 sites (=0.54×54) are occupied out of the maximal 54 sites available for oxime binding. Increasing the [2-PAM]/[G5-GA] ratio to 120 leads to a higher θ value of 0.71 (≈38 oxime molecules bound), though this level appears to be already saturated at the lower ratio ([2-PAM]/[G5-GA] ratio = 100). The other analysis performed for the same G5-GA/2-PAM complex but measured in the PBS condition shows a similar trend with the maximal fractional occupancy slightly higher (θ = 0.79 at [2-PAM]/[G5-GA] ratio =100). Thus, this ionic condition (PBS, I = 0.15) affects the loading capacity to some extent. For example, 2-PAM molecules bound slightly more in PBS than D_2O by up to 5 drug molecules per dendrimer otherwise under the identical condition. We believe that such different loading capacity might be attributable to the variation in the structure and configuration of the G5-GA dendrimer which occurs in response to external factors such as solvent, pH, and ionic strength.[1,61−63] It might be possible that salt ions can open up dendritic branches by interrupting their intramolecular networks within the dendrimer structure, a mechanism that might decrease the extent of unfavorable steric congestion arising from drug binding.

The plot in Figure 9B also illustrates that the fraction of obidoxime molecules bound to the G5-GA dendrimer increases as a function of the [obidoxime]/[G5-GA] ratio, and it reaches the saturation value at the range of [obidoxime]/[G5-GA] = 100−120. However unlike 2-PAM, obidoxime has two identical

dx.doi.org/10.1021/jp305867v | J. Phys. Chem. B 2012, 116, 10387−10397

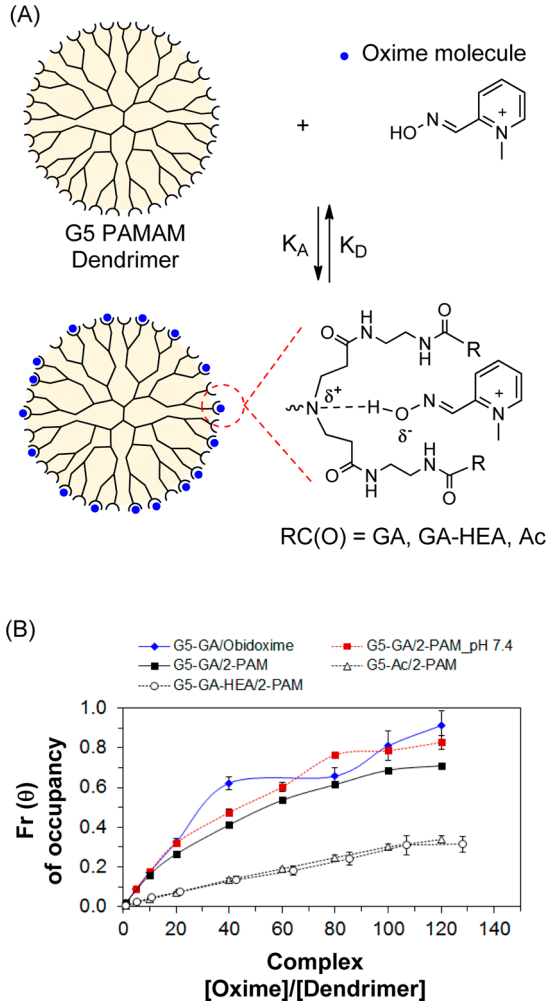

Figure 9. (A) A proposed model for the binding of oxime molecules to G5 PAMAM dendrimers (G5-GA, G5-Ac, G5-GA-HEA). (B) The fraction (θ) of receptor occupancy is plotted as a function of the molar ratio of oxime molecules (2-PAM or obidoxime) added to the dendrimer. The number of receptor units per dendrimer is estimated as 54 (=108/2). The value of fractional occupancy is directly calculated from the number of bound oxime molecules per dendrimer carrier (=54 × θ). The error bars in (B) represent standard deviations calculated from the mean value.

aldoxime moieties linked in a C_2 symmetry, and thus has two possible modes of interaction: (i) the monovalent one where only one of the two aldoxime moieties involves in the binding, and (ii) the bivalent one where both aldoxime moieties involve simultaneously in the binding. Considering the earlier analysis performed for the dendrimer side (Figures 3C and 5C), the chemical shift changes (Δ) observed at the tertiary amine branches reach the maximal level at the similar ratio of [obidoxime]/[G5-GA] ≈ 80−100. Thus, the [obidoxime]/[G5-GA] ratio that reaches the binding saturation is consistent regardless of the analysis based on either the obidoxime side (θ; Figure 9B) or the dendrimer counterpart (Δ; Figures 3C and 5C). Combination of such analyses suggests 1:1 binding stoichiometry between the obidoxime molecule and the dendrimer site. This supports a model for the functionally monovalent interaction by the obidoxime molecule (Figure 6B).

Affinity and Cooperativity. In Figure 9, we discussed that the fraction of drug occupied sites is correlated, in large part, with the surface functionality of the dendrimer. The maximal fractional occupancy is much lower for neutrally modified dendrimers such as G5-Ac and G5-GA-HEA than the negatively charged dendrimer G5-GA. We were interested in determining if this global binding capacity relates to the affinity of individual binding events. We performed the Scatchard analysis for each drug complex by plotting of $\theta/[\text{oxime}]_{\text{free}}$ against θ as illustrated by the G5-GA/2-PAM complex (Figure 10A). It

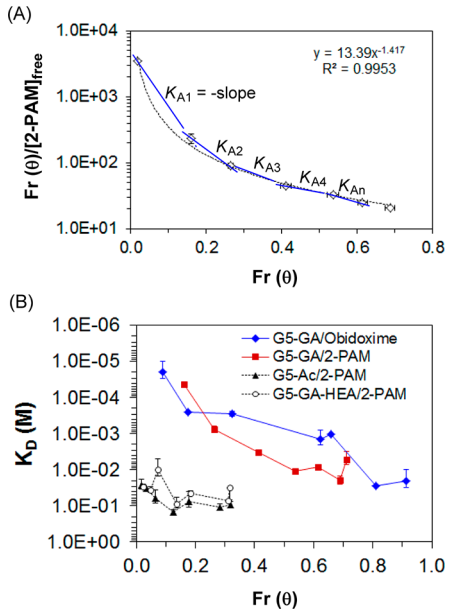

Figure 10. Quantitative analysis for the complexation of G5 dendrimer with two oxime drugs. (A) Scatchard analysis for the complex of 2-PAM molecules with the G5-GA dendrimer as a model multivalent system. This Scatchard plot is derived from the ^{1}H NMR titration experiments in D_2O described earlier. (B) Plots of steady-state dissociation constants (K_D = $1/K_A$) for the oxime−dendrimer complexes as a function of the fraction of receptor occupancy (θ).

shows nonlinear decay, indicating that association constant (K_A = −slope) varies as a function of fractional occupancy (θ). Thus, instead of calculating the average affinity, we estimated affinity distribution as a function of θ as summarized in Figure 10B. First, the highest binding affinity of 2-PAM is greater for G5-GA ($K_D \geq 10^{-5}$ M) by up to 3 orders of magnitude than G5-Ac or G5-GA-HEA ($K_D \geq 10^{-2}$ M). Second, affinities are slightly greater for obidoxime than for 2-PAM for G5-GA complexes compared at the identical fraction of occupancy. It suggests possible contribution by certain structural elements of the obidoxime molecule such as the ether linker and/or the second pyridinium cation. Third, the affinities are higher where fractions of occupancy are lower ($K_D \geq 10^{-5}$ M at $\theta \leq 0.2$), and thus are inversely correlated with the fractional occupancy. This nonlinear distribution of affinity indicates a negative cooperativity that is likely the result of repulsive interaction arising from successive binding events. In order to assess a quantitative index for such negative cooperativity, we calculated the Hill coefficient (n) for each drug complex made with G5-GA (Figure S8 in the Supporting Information). Values of the Hill coefficient determined for the two G5-GA complexes are 0.66 (2-PAM) and 0.68 (obidoxime). Thus, the result of the Hill analysis points to negative cooperativity ($n < 1$) for the binding with 2-PAM or obidoxime molecules rather than either noncooperativity ($n = 1$) or positive cooperativity ($n > 1$).

dx.doi.org/10.1021/jp305867v | J. Phys. Chem. B 2012, 116, 10387−10397

We hypothesize that this negative cooperative effect might be attributable to the mechanism of steric congestion by which multiple binding events, though all based on the identical mode of interaction, lead to the distribution of the binding affinity. This negative cooperativity is implicated in a range of multivalent receptor systems. As a classical example found in antibody−antigen recognition processes, an IgM antibody molecule (decavalent) shows disparity in the affinity constants for its 10 antigen-recognition sites despite their structural identity.[64,65] Our observation is also in line with certain synthetic systems such as the metallodendrimers that catalyze the reactions but under steric influence.[6] However, in some other dendrimer-based catalytic reactions, the substrate binding is known to be less sensitive to the steric effect due to its rapid turnover during the catalytic cycle.[5,8]

■ CONCLUSIONS

This present study provides unique insights that characterize the interaction occurring between a nanoscale polymer carrier and small molecule drugs. We employed surface-modified dendrimers derived from a fifth generation PAMAM dendrimer and investigated their interaction with oxime-based small molecules essential for treatment of OP poisoning. Each drug molecule binds to a tertiary amine site proximal to the dendrimer surface through a specific oxime−amine interaction rather than through a nonselective encapsulation into the dendritic core. Individual drug binding events that constitute the global interaction occur in a negatively cooperative manner as the number of complexed drug molecules increases. This study raises the possibility that steric congestion may be responsible for the variations in binding affinities seen with oximes in this system.

■ ASSOCIATED CONTENT

Supporting Information

In vitro cytotoxicity data, GPC traces of modified PAMAM dendrimers, full NMR spectra for the NMR experiments (1D titration, COSY, NOESY, DOSY), additional plots for Δ values (1D titration), and Hill plots. This material is available free of charge via the Internet at http://pubs.acs.org.

■ AUTHOR INFORMATION

Corresponding Author

*Phone: (734) 615-0618 (S.K.C.); (734) 647-2777 (J.R.B.). Fax: (734) 615-0621 (S.K.C.); (734) 615-2506 (J.R.B.). E-mail: skchoi@umich.edu (S.K.C.); jbakerjr@umich.edu (J.R.B.).

Notes

The authors declare no competing financial interest.

■ ACKNOWLEDGMENTS

This work has been supported by the Federal funds from the Defense Advanced Research Projects Agency−DOD, under award W911NF-07-1-0437. We thank Mr. Ankur Desai for performing the GPC experiments.

■ REFERENCES

(1) Tomalia, D. A.; Naylor, A. M.; William, A.; Goddard, I. *Angew. Chem., Int. Ed. Engl.* **1990**, *29*, 138−175.
(2) Bosman, A. W.; Janssen, H. M.; Meijer, E. W. *Chem. Rev. (Washington, DC, U.S.)* **1999**, *99*, 1665−1688.
(3) Caminade, A.-M.; Majoral, J.-P. *Acc. Chem. Res.* **2004**, *37*, 341−348.
(4) van Heerbeek, R.; Kamer, P. C. J.; van Leeuwen, P. W. N. M.; Reek, J. N. H. *Chem. Rev. (Washington, DC, U.S.)* **2002**, *102*, 3717−3756.
(5) Francavilla, C.; Drake, M. D.; Bright, F. V.; Detty, M. R. *J. Am. Chem. Soc.* **2000**, *123*, 57−67.
(6) Kleij, A. W.; Gossage, R. A.; Jastrzebski, J. T. B. H.; Boersma, J.; van Koten, G. *Angew. Chem., Int. Ed. Engl.* **2000**, *39*, 176−178.
(7) Astruc, D.; Boisselier, E.; Ornelas, C. t. *Chem. Rev. (Washington, DC, U.S.)* **2010**, *110*, 1857−1959.
(8) Breinbauer, R.; Jacobsen, E. N. *Angew. Chem., Int. Ed. Engl.* **2000**, *39*, 3604−3607.
(9) Choi, S. K.; Leroueil, P.; Li, M.-H.; Desai, A.; Zong, H.; Van Der Spek, A. F. L.; Baker, J. R., Jr. *Macromolecules* **2011**, *44*, 4026−4029.
(10) Hecht, S.; Fréchet, J. M. J. *Angew. Chem., Int. Ed. Engl.* **2001**, *40*, 74−91.
(11) Gomez, M. V.; Guerra, J.; Velders, A. H.; Crooks, R. M. *J. Am. Chem. Soc.* **2009**, *131*, 341−350.
(12) Shi, X.; Lee, I.; Chen, X.; Shen, M.; Xiao, S.; Zhu, M.; Baker, J. R.; Wang, S. H. *Soft Matter* **2010**, *6*, 2539−2545.
(13) Zhang, M.; Guo, R.; Wang, Y.; Cao, X.; Shen, M.; Shi, X. *Int. J. Nanomed.* **2011**, *6*, 2337−2349.
(14) Majoros, I. J.; Thomas, T. P.; Mehta, C. B.; Baker, J. R., Jr. *J. Med. Chem.* **2005**, *48*, 5892−5899.
(15) Hong, S.; Leroueil, P. R.; Majoros, I. J.; Orr, B. G.; Baker, J. R., Jr.; Banaszak Holl, M. M. *Chem. Biol. (Cambridge, MA, U.S.)* **2007**, *14*, 107−115.
(16) Li, M.-H.; Choi, S. K.; Thomas, T. P.; Desai, A.; Lee, K.-H.; Kotlyar, A.; Banaszak Holl, M. M.; Baker, J. R., Jr. *Eur. J. Med. Chem.* **2012**, *47*, 560−572.
(17) Thomas, T. P.; Choi, S. K.; Li, M.-H.; Kotlyar, A.; Baker, J. R., Jr. *Bioorg. Med. Chem. Lett.* **2010**, *20*, 5191−5194.
(18) Thomas, T. P.; Goonewardena, S. N.; Majoros, I. J.; Kotlyar, A.; Cao, Z.; Leroueil, P. R.; Baker, J. R. *Arthritis Rheum.* **2011**, *63*, 2671−2680.
(19) Kensinger, R. D.; Yowler, B. C.; Benesi, A. J.; Schengrund, C.-L. *Bioconjugate Chem.* **2004**, *15*, 349−358.
(20) Yang, H.; Zhuang, Y.; Sun, Y.; Dai, A.; Shi, X.; Wu, D.; Li, F.; Hu, H.; Yang, S. *Biomaterials* **2011**, *32*, 4584−4593.
(21) Broeren, M. A. C.; de Waal, B. F. M.; van Genderen, M. H. P.; Sanders, H. M. H. F.; Fytas, G.; Meijer, E. W. *J. Am. Chem. Soc.* **2005**, *127*, 10334−10343.
(22) Marchioni, F.; Venturi, M.; Credi, A.; Balzani, V.; Belohradsky, M.; Elizarov, A. M.; Tseng, H.-R.; Stoddart, J. F. *J. Am. Chem. Soc.* **2003**, *126*, 568−573.
(23) Hu, J.; Cheng, Y.; Wu, Q.; Zhao, L.; Xu, T. *J. Phys. Chem. B* **2009**, *113*, 10650−10659.
(24) Cheng, Y.; Li, Y.; Wu, Q.; Zhang, J.; Xu, T. *Eur. J. Med. Chem.* **2009**, *44*, 2219−2223.
(25) Kojima, C.; Kono, K.; Maruyama, K.; Takagishi, T. *Bioconjugate Chem.* **2000**, *11*, 910−917.
(26) Medina, S. H.; El-Sayed, M. E. H. *Chem. Rev. (Washington, DC, U.S.)* **2009**, *109*, 3141−3157.
(27) Patri, A. K.; Kukowska-Latallo, J. F.; Baker, J. J. R. *Adv. Drug Delivery Rev.* **2005**, *57*, 2203−2214.
(28) Boas, U.; Söntjens, S. H. M.; Jensen, K. J.; Christensen, J. B.; Meijer, E. W. *ChemBioChem* **2002**, *3*, 433−439.
(29) Giri, J.; Diallo, M. S.; Simpson, A. J.; Liu, Y.; Goddard, W. A.; Kumar, R.; Woods, G. C. *ACS Nano* **2011**, *5*, 3456−3468.
(30) Pavan, G. M.; Posocco, P.; Tagliabue, A.; Maly, M.; Malek, A.; Danani, A.; Ragg, E.; Catapano, C. V.; Pricl, S. *Chem.—Eur. J.* **2010**, *16*, 7781−7795.
(31) Kukowska-Latallo, J. F.; Bielinska, A. U.; Johnson, J.; Spindler, R.; Tomalia, D. A.; Baker, J. R. *Proc. Natl. Acad. Sci. U.S.A.* **1996**, *93*, 4897−4902.
(32) Santos, J. L.; Pandita, D.; Rodrigues, J. o.; Pêgo, A. P.; Granja, P. L.; Balian, G.; Tomás, H. *Mol. Pharm.* **2010**, *7*, 763−774.
(33) Luo, D.; Haverstick, K.; Belcheva, N.; Han, E.; Saltzman, W. M. *Macromolecules* **2002**, *35*, 3456−3462.

(34) Wang, M.; Gong, X.; Hu, J.; Yu, Y.; Chen, Q.; Cheng, Y. *J. Phys. Chem. B* **2011**, *115*, 12728−12735.
(35) Zimmerman, S. C.; Zeng, F.; Reichert, D. E. C.; Kolotuchin, S. V. *Science (Washington, DC, U.S.)* **1996**, *271*, 1095−1098.
(36) Castro, R.; Cuadrado, I.; Alonso, B.; Casado, C. M.; Morán, M.; Kaifer, A. E. *J. Am. Chem. Soc.* **1997**, *119*, 5760−5761.
(37) Yang, K.; Weng, L.; Cheng, Y.; Zhang, H.; Zhang, J.; Wu, Q.; Xu, T. *J. Phys. Chem. B* **2011**, *115*, 2185−2195.
(38) Percec, V.; Mitchell, C. M.; Cho, W.-D.; Uchida, S.; Glodde, M.; Ungar, G.; Zeng, X.; Liu, Y.; Balagurusamy, V. S. K.; Heiney, P. A. *J. Am. Chem. Soc.* **2004**, *126*, 6078−6094.
(39) Percec, V.; Dulcey, A. E.; Balagurusamy, V. S. K.; Miura, Y.; Smidrkal, J.; Peterca, M.; Nummelin, S.; Edlund, U.; Hudson, S. D.; Heiney, P. A.; Duan, H.; Magonov, S. N.; Vinogradov, S. A. *Nature (London, U.K.)* **2004**, *430*, 764−768.
(40) Edery, H.; Schatzberg-Porath, G. *Science (Washington, DC, U.S.)* **1958**, *128*, 1137−1138.
(41) Cohen, S.; Ashani, Y. *J. Med. Chem.* **1971**, *14*, 621−626.
(42) Jovanović, D. *Arch. Toxicol.* **1989**, *63*, 416−418.
(43) Han, J.; Lim, S.-J.; Lee, M.-K.; Kim, C.-K. *Drug Delivery* **2001**, *8*, 125−134.
(44) Morgan, M. T.; Nakanishi, Y.; Kroll, D. J.; Griset, A. P.; Carnahan, M. A.; Wathier, M.; Oberlies, N. H.; Manikumar, G.; Wani, M. C.; Grinstaff, M. W. *Cancer Res.* **2006**, *66*, 11913−11921.
(45) Kukowska-Latallo, J. F.; Candido, K. A.; Cao, Z.; Nigavekar, S. S.; Majoros, I. J.; Thomas, T. P.; Balogh, L. P.; Khan, M. K.; Baker, J. R., Jr. *Cancer Res.* **2005**, *65*, 5317−5324.
(46) Choi, S. K.; Thomas, T.; Li, M.; Kotlyar, A.; Desai, A.; Baker, J. R., Jr. *Chem. Commun. (Cambridge, U.K.)* **2010**, *46*, 2632−2634.
(47) Witte, A. B.; Timmer, C. M.; Gam, J. J.; Choi, S. K.; Banaszak Holl, M. M.; Orr, B. G.; Baker, J. R.; Sinniah, K. *Biomacromolecules* **2012**, *13*, 507−516.
(48) Fielding, L. *Prog. Nucl. Magn. Reson. Spectrosc.* **2007**, *51*, 219−242.
(49) Macomber, R. S. *J. Chem. Educ.* **1992**, *69*, 375−378.
(50) Alvarado, E. *Diffusino experiments with Vnmrj 2.2C and 2.2D.* University of Michigan: Ann Arbor, 2010; http://www.umich.edu/~chemnmr/docs/diffusion.pdf.
(51) Stejskal, E. O.; Tanner, J. E. *J. Chem. Phys.* **1965**, *42*, 288−292.
(52) Thomas, T. P.; Majoros, I.; Kotlyar, A.; Mullen, D.; Banaszak Holl, M. M.; Baker, J. R. *Biomacromolecules* **2009**, *10*, 3207−3214.
(53) Roehm, N. W.; Rodgers, G. H.; Hatfield, S. M.; Glasebrook, A. L. *J. Immunol. Methods* **1991**, *142*, 257−265.
(54) Leroueil, P. R.; Hong, S.; Mecke, A.; Baker, J. R.; Orr, B. G.; Banaszak Holl, M. M. *Acc. Chem. Res.* **2007**, *40*, 335−342.
(55) Karljikovic-Rajic, K.; Stankovic, B. *J. Pharm. Biomed. Anal.* **1990**, *8*, 705−709.
(56) Cakara, D.; Kleimann, J.; Borkovec, M. *Macromolecules* **2003**, *36*, 4201−4207.
(57) Diallo, M. S.; Christie, S.; Swaminathan, P.; Balogh, L.; Shi, X.; Um, W.; Papelis, C.; Goddard, W. A.; Johnson, J. H. *Langmuir* **2004**, *20*, 2640−2651.
(58) Spöhrer, U.; Eyer, P. *J. Chromatogr., A* **1995**, *693*, 55−61.
(59) Pelta, M. D.; Barjat, H.; Morris, G. A.; Davis, A. L.; Hammond, S. J. *Magn. Reson. Chem.* **1998**, *36*, 706−714.
(60) Dubin, P. L.; Edwards, S. L.; Kaplan, J. I.; Mehta, M. S.; Tomalia, D.; Xia, J. *Anal. Chem.* **1992**, *64*, 2344−2347.
(61) Maiti, P. K.; Cagin, T.; Lin, S. T.; Goddard, W. A., III *Macromolecules* **2005**, *38*, 979−991.
(62) Liu, Y.; Bryantsev, V. S.; Diallo, M. S.; Goddard, W. A., III *J. Am. Chem. Soc.* **2009**, *131*, 2798−2799.
(63) Porcar, L.; Hong, K.; Butler, P. D.; Herwig, K. W.; Smith, G. S.; Liu, Y.; Chen, W.-R. *J. Phys. Chem. B* **2010**, *114*, 1751−1756.
(64) Edberg, S. C.; M. Bronson, P.; Van Oss, C. J. *Immunochemistry* **1972**, *9*, 273−288.
(65) Goldstein, B. *Biophys. Chem.* **1975**, *3*, 363−367.